Electronic Supplementary Material (ESI) for Physical Chemistry Chemical Physics.

Effect of Alkali Metal Cations on Network Rearrangement in Polyisoprene Ionomers

Yohei Miwa,[1, †,] Koki Hasegawa,[1] Taro Udagawa,[1] Yu Shinke,[2] and Shoichi Kutsumizu[1]*

[1]Department of Chemistry and Biomolecular Science, Faculty of Engineering, Gifu University, Yanagido, Gifu 501-1193, Japan.

[2]The Yokohama Rubber Co., Ltd., Hiratsuka, 254-8601, Japan.

[†]PRESTO, Japan Science and Technology Agency.

*Author to whom correspondence should be addressed.

E-mail: y_miwa@gifu-u.ac.jp

Table of Contents

Fig. S8. DSC traces for second heating process of the indicated samples.

Fig. S9. Temperature dependence of (A) storage modulus (G') and (B) loss modulus (G'') for PI-Na measured at 1 Hz. Relaxations assigned to the network rearrangement are indicated with arrows. The relaxation temperature decreases with the moisture absorption of the sample.

Fig. S10. Temperature dependences of saturation factor, S, for PI-Na spin-probed with 4-carboxy-TEMPO at different concentrations (4×10^{-8} mol g^{-1} and 6×10^{-8} mol g^{-1}) and for PI-Na spin-probed with 5DSA at 6×10^{-8} mol g^{-1}. $T_{g,ESR}$ of each sample is indicated with arrow. Each plot is vertically shifted to avoid overlapping.

DFT calculation

To assess the accuracy of the calculation, we have performed some preliminary calculations. Since we mainly focused on the cation–π interaction, simple systems, Li^+···ethylene and Cs^+···ethylene complexes, were chosen as the model systems for the preliminary calculation. First, geometry-optimization calculation was performed by M06/6-31G(d,p), 6-31+G(d,p), 6-311+G(d,p), and aug-cc-pVTZ methods. As shown in **Fig. S1**, the C_{2v} optimized structure was obtained. The cation–π distance and interaction energy are listed in Table S1. The cation–π distance is almost unchanged by adopting larger basis sets. In addition, the M06/6-31G(d,p) calculation sufficiently reproduced the interaction energy obtained by the most accurate M06/aug-cc-pVTZ calculation.

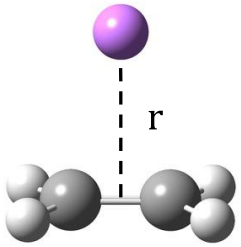

Fig. S1. Optimized structure (C_{2v}) of Li^+(Cs^+)···ethylene complex.

Table S1. Cation–π distance [Å] and interaction energy (IE)[a] [kcal/mol] in Li^+–ethylene and Cs^+–ethylene complexes.

	Li^+···ethylene		Cs^+···ethylene	
	r(Li^+–π)	IE[a]	r(Cs^+–π	IE[a]
6-31G(d,p)	2.319	-23.0	3.676	-4.8
6-31+G(d,p)	2.326	-20.0	3.687	-3.6
6-311+G(d,p)	2.302	-19.5	3.676	-5.3
aug-cc-pVTZ	2.294	-20.7	3.636	-5.9

[a] IE is defined as $\mathrm{IE} = E(\text{cation–ethylene}) - \{E(\text{cation}) + E(\text{ethylene})\}$.

We further checked the validity of the use of 6-31G(d,p) basis set by drawing the potential energy curve along cation–π distance. **Fig. S2** shows the potential energy curves for cation–ethylene complexes. Clearly, the M06/6-31G(d,p) and the M06/aug-cc-pVTZ potential energy curves are similar to each other for both Li^+–ethylene and Cs^+–ethylene complexes.

These preliminary calculations clearly demonstrated that the M06/6-31G(d,p) method is accurate enough for analyzing cation–π complexes.

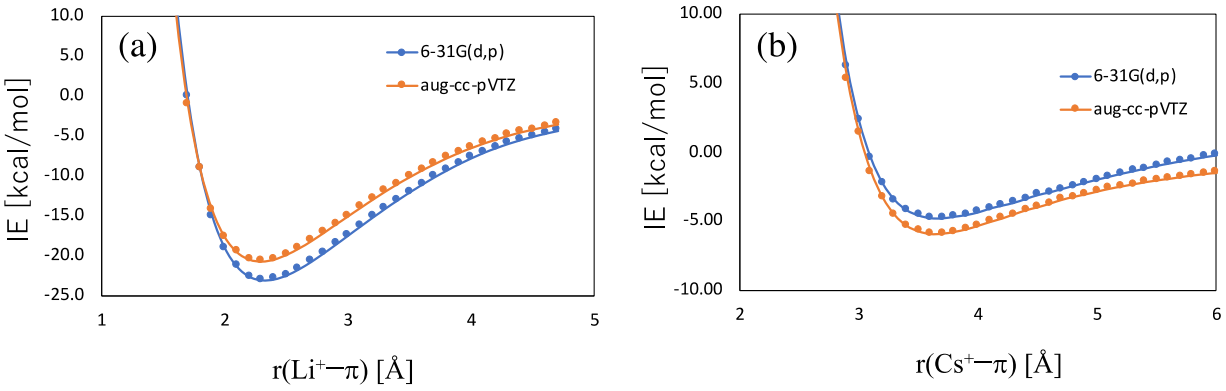

Fig. S2. Potential energy curve along cation–π distance for (a) Li^+···ethylene and (b) Cs^+···ethylene complexes obtained by M06/6-31G(d,p) and M06/aug-cc-pVTZ calculations.

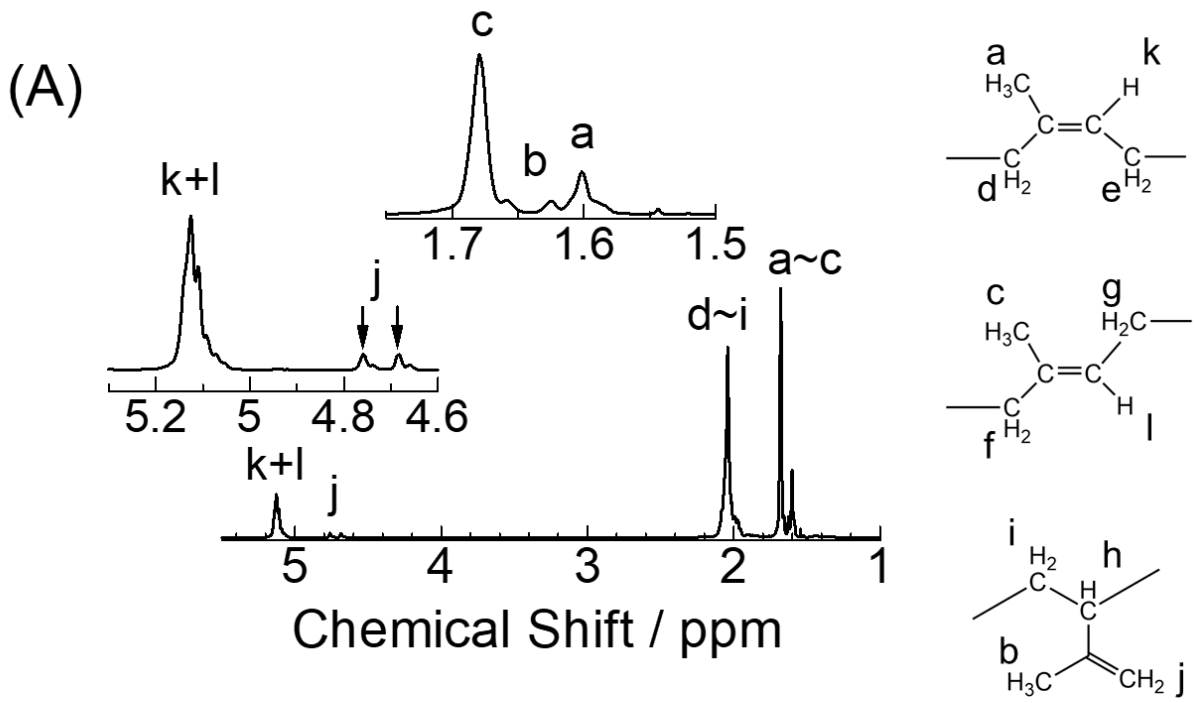

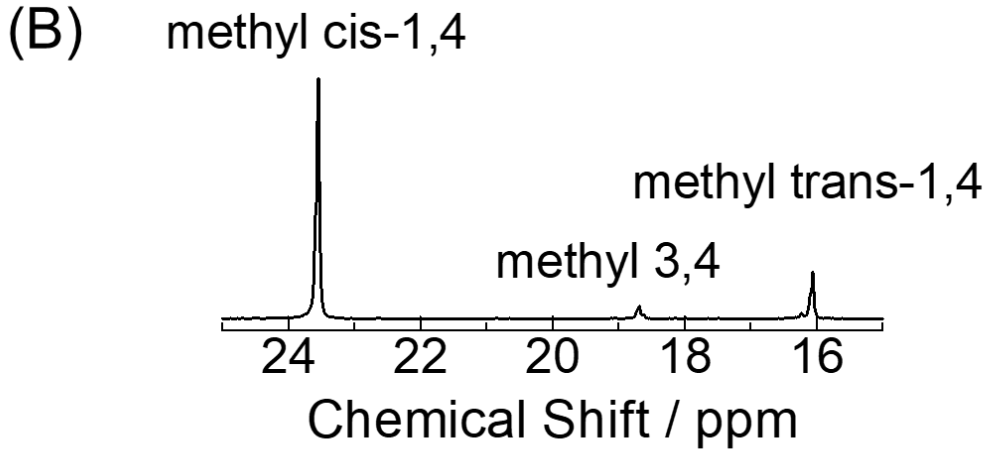

Fig. S3. (A) ^{1}H-NMR and (B) ^{13}C-NMR spectra for PI used in this work.

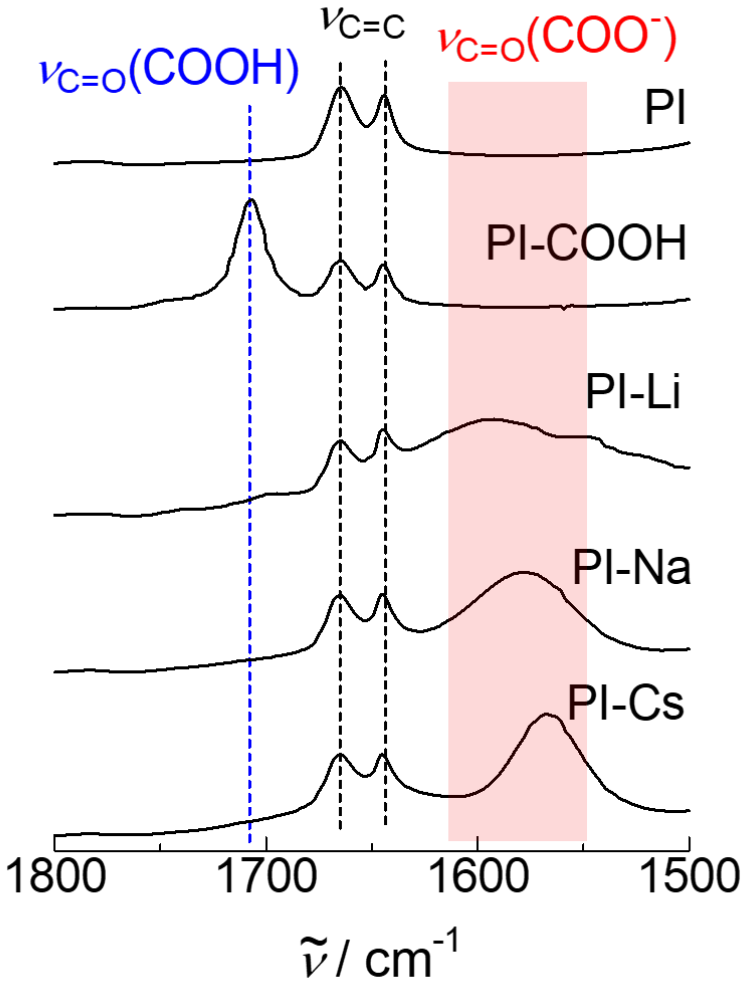

Fig. S4. FT–IR bands for ν(C=O) of carboxy and ν(O−C−O$^-$) of sodium carboxylate for the samples are indicated.

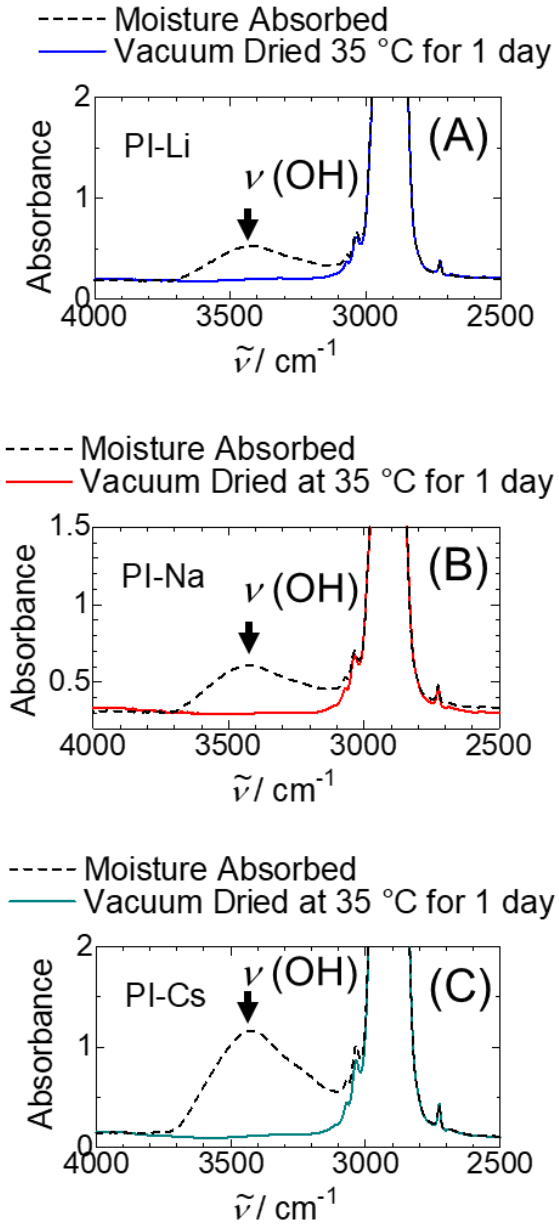

Fig. S5. FT–IR band for ν(O−H) of water in the indicates samples. This band is clearly shown in the moisture absorbed samples. On the other hands, the ν(O−H) band are completely disappeared after vacuum drying at 35 °C for 1 day. This demonstrates complete drying of these samples by this procedure.

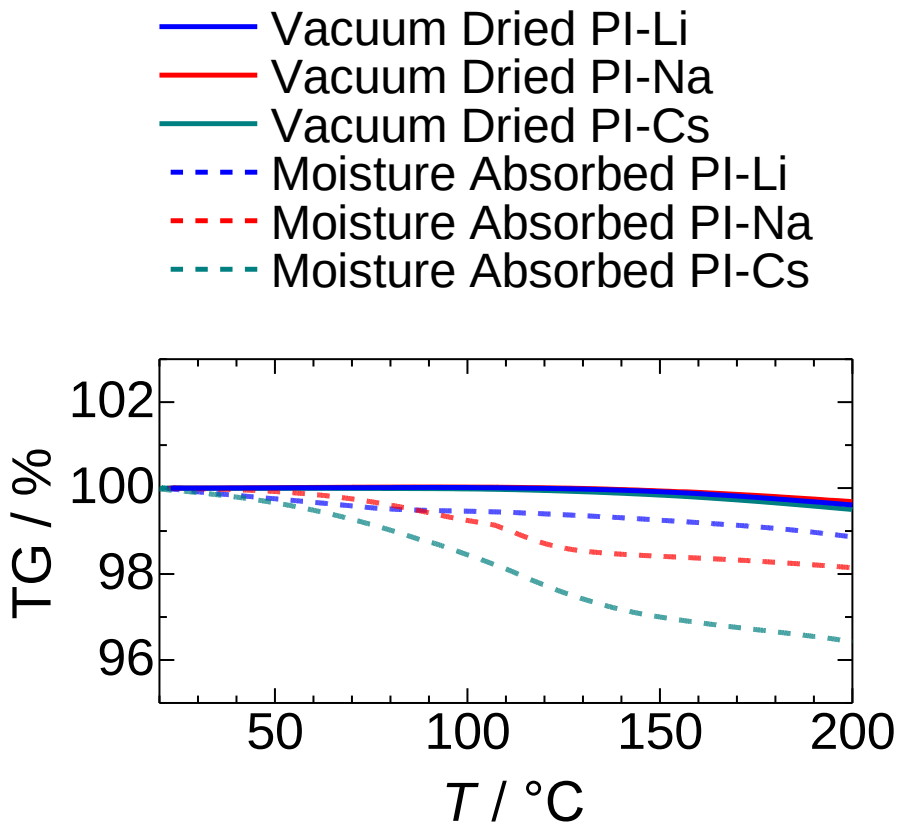

Fig. S6. TG results for the indicates samples. The weight loss from the water detachment was observed for the moisture absorbed samples. The TG curves for the samples vacuum dried at 35 °C for 2 days are overlapped with each other.

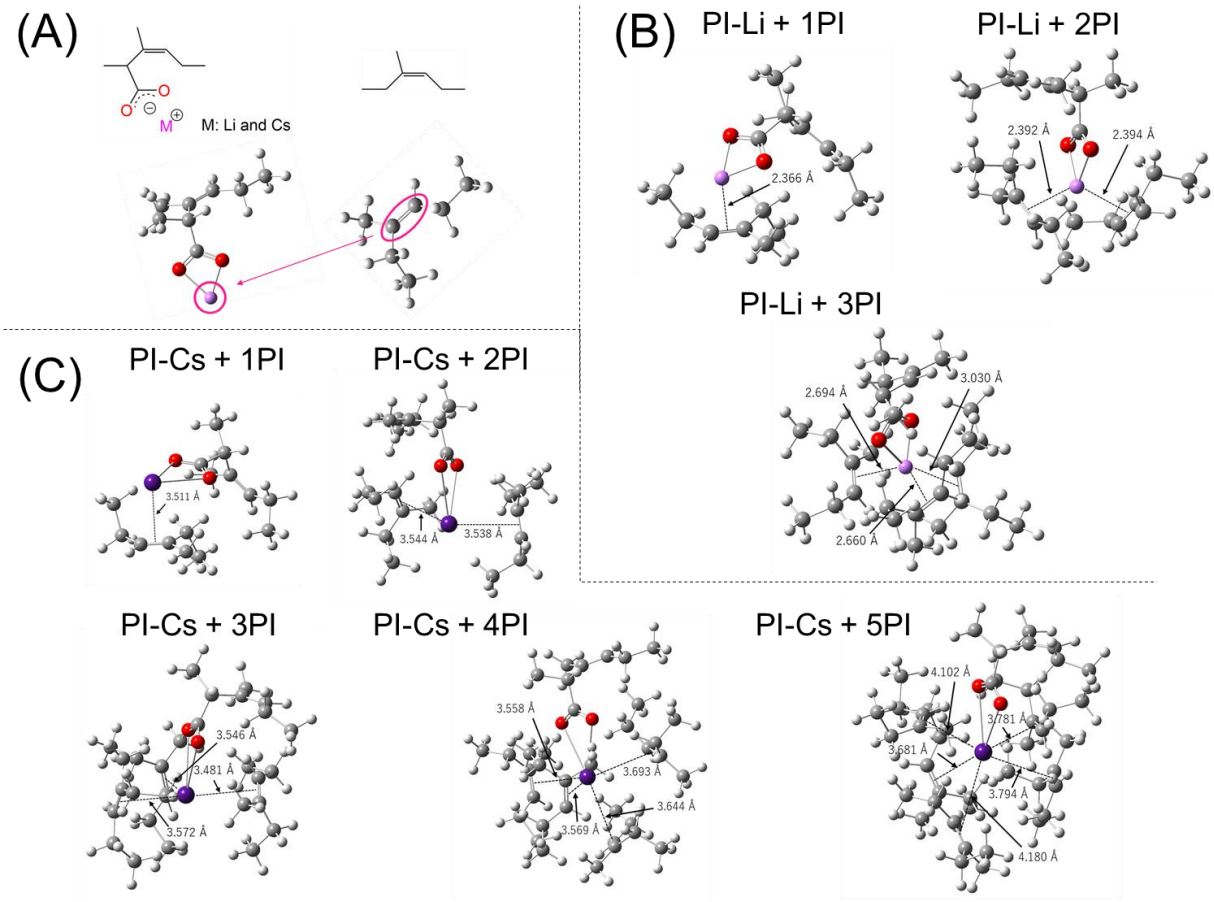

Fig. S7. DFT calculation results for cation-π interaction between double bond in the PI unit and Li^+ and Cs^+. (A) Model segments used for the calculation. Most stable structure for each coordination in (B) PI-Li+*n*PI and (C) PI-Cs+*n*PI.

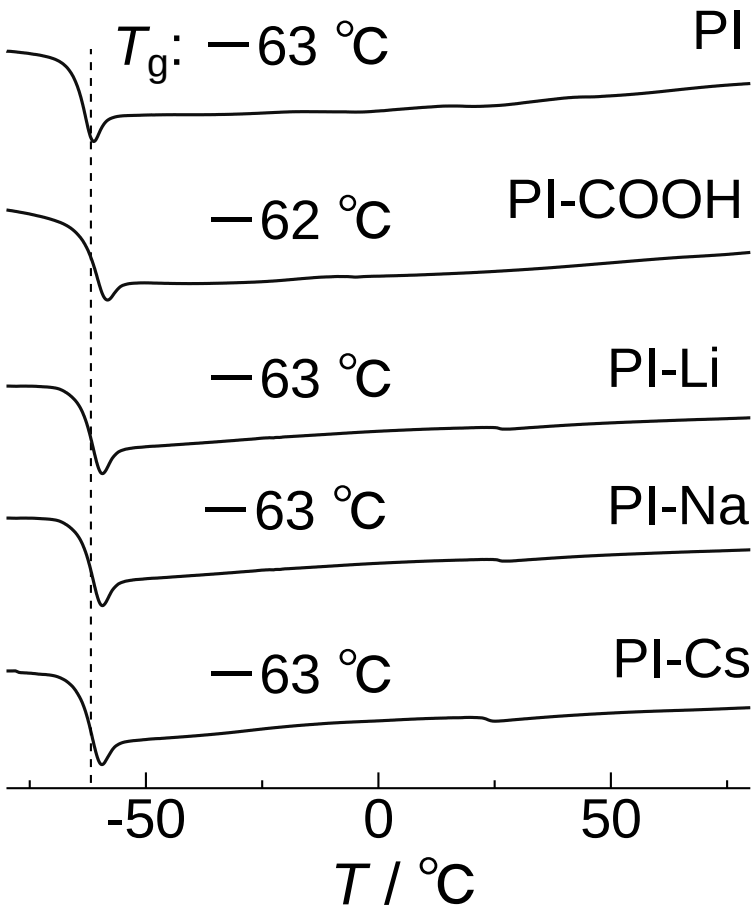

Fig. S8. DSC traces for second heating process of the indicated samples.

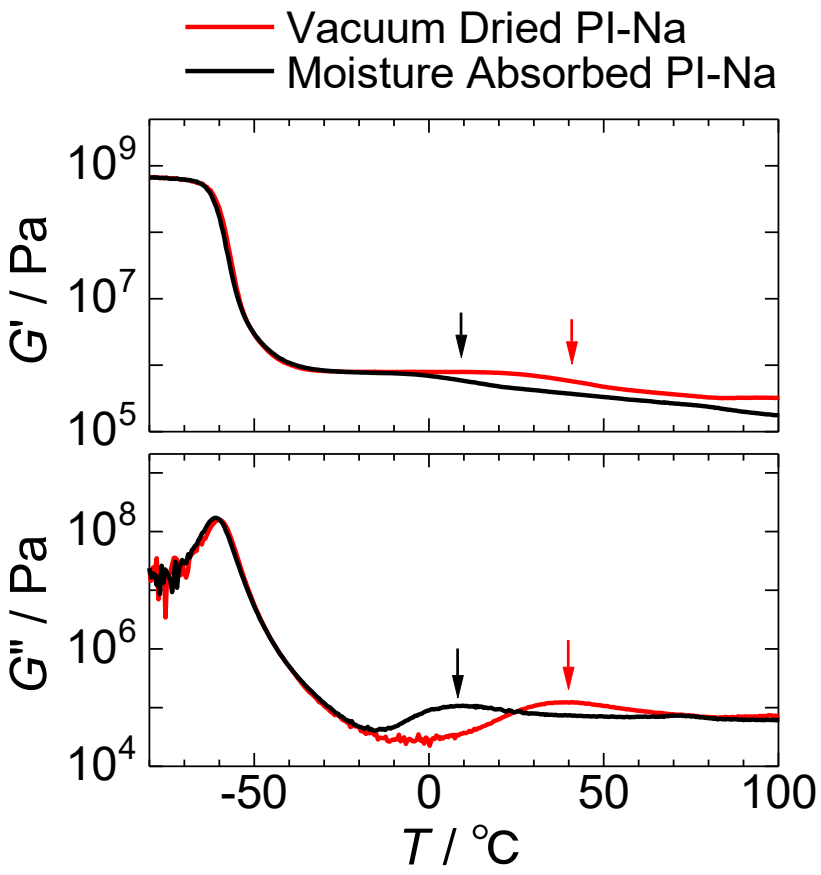

Fig. S9. Temperature dependence of (A) storage modulus (G') and (B) loss modulus (G'') for PI-Na measured at 1 Hz. Relaxations assigned to the network rearrangement are indicated with arrows. The relaxation temperature decreases with the moisture absorption of the sample.

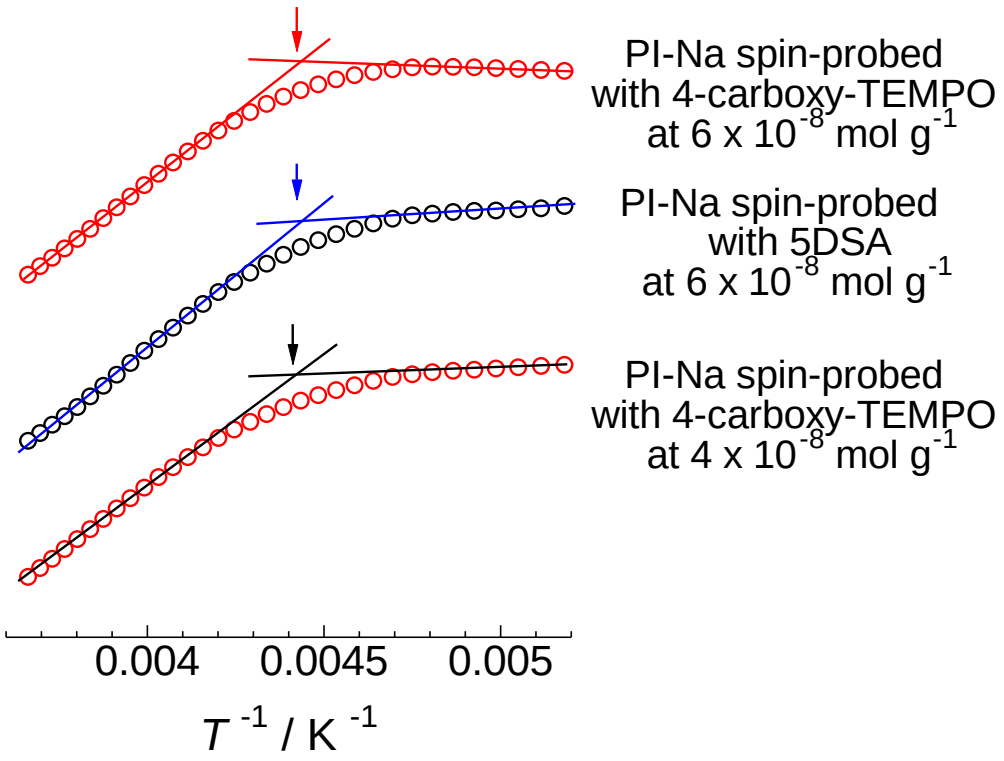

Fig. S10. Temperature dependences of saturation factor, *S*, for PI-Na spin-probed with 4-carboxy-TEMPO at different concentrations (4 $\times 10^{-8}$ mol g^{-1} and 6 $\times 10^{-8}$ mol g^{-1}) and for PI-Na spin-probed with 5DSA at 6 $\times 10^{-8}$ mol g^{-1}. $T_{g,ESR}$ of each sample is indicated with arrow. Each plot is vertically shifted to avoid overlapping.